Cell, Vol. 118, 555–566, September 3, 2004, Copyright ©2004 by Cell Press

Chromatin Architecture of the Human Genome: Gene-Rich Domains Are Enriched in Open Chromatin Fibers

Nick Gilbert,[1,3] Shelagh Boyle,[1,3] Heike Fiegler,[2] Kathryn Woodfine,[2] Nigel P. Carter,[2] and Wendy A. Bickmore[1,*]
[1]MRC Human Genetics Unit
Edinburgh
EH4 2XU
Scotland
[2]The Wellcome Trust Sanger Institute
Hinxton
Cambridge CB10 1SA
United Kingdom

Summary

We present an analysis of chromatin fiber structure across the human genome. Compact and open chromatin fiber structures were separated by sucrose sedimentation and their distributions analyzed by hybridization to metaphase chromosomes and genomic microarrays. We show that compact chromatin fibers originate from some sites of heterochromatin (C-bands), and G-bands (euchromatin). Open chromatin fibers correlate with regions of highest gene density, but not with gene expression since inactive genes can be in domains of open chromatin, and active genes in regions of low gene density can be embedded in compact chromatin fibers. Moreover, we show that chromatin fiber structure impacts on further levels of chromatin condensation. Regions of open chromatin fibers are cytologically decondensed and have a distinctive nuclear organization. We suggest that domains of open chromatin may create an environment that facilitates transcriptional activation and could provide an evolutionary constraint to maintain clusters of genes together along chromosomes.

Introduction

Modulation of chromatin structure is central to the regulation of gene expression. This is best understood at the level of the nucleosome and its modifications. For example, acetylation and methylation of lysine residues in histones H3 and H4 have been correlated to either active transcription or gene repression, depending on the nature of the modification (Fischle et al., 2003). Variant histones also impact on nucleosome structure and function (Fan et al., 2002; McKittrick et al., 2004). However, beyond the nucleosome itself, there are other structural states of chromatin that will influence how the underlying DNA sequence is read. Active and silent regions are often considered to have "open" and "closed" chromatin structures, respectively (Felsenfeld and Groudine, 2003; Vermaak et al., 2003). However, biophysical evidence for different chromatin fiber structures, which might equate with these concepts, has been lacking.

*Correspondence: w.bickmore@hgu.mrc.ac.uk
[3]These authors contributed equally to this work.

At low salt concentrations nucleosome arrays can form 10 nm fibers (Thoma et al., 1979; Wolffe, 1998) that undergo a conformational change to a 30 nm fiber with increasing salt (Greulich et al., 1987). However, it is not understood how nucleosome arrays are arranged into the 30 nm fiber (Thoma et al., 1979; McGhee et al., 1983; Woodcock et al., 1984; van Holde and, Zlatanova, 1996; Wolffe, 1998). 30 nm chromatin fibers are detected in cells by low angle X-ray diffraction (Langmore and Paulson, 1983), but by electron microscopy a large proportion of mammalian chromatin appears packaged into levels beyond this, visualized as 60 to 130 nm "chromonema" fibers (Belmont and Bruce, 1994). Unfolding and decondensation of chromatin fibers is seen by light microscopy when transcriptional regulators are artificially targeted to the mammalian genome (Tumbar et al., 1999; Tsukamoto et al., 2000; Muller et al., 2001; Ye et al., 2001; Nye et al., 2002). Recently, decondensation of the endogenous murine *HoxB* locus has been shown to accompany the induction of transcription (Chambeyron and Bickmore, 2004).

The structure of the 30 nm chromatin fiber has been assayed by sucrose gradient sedimentation, but at only a few loci. In chicken erythrocytes, chromatin from the (active) β-*globin* locus sediments more slowly than bulk chromatin or a nonexpressed gene, whereas it sediments with bulk chromatin in nonexpressing cells (Kimura et al., 1983; Fisher and Felsenfeld, 1986; Caplan et al., 1987). Chromatin from a plasmid-borne induced gene in yeast sediments slower than that from the uninduced locus (Kim and Clark, 2002). Hence, it has been suggested that the chromatin fiber unfolds upon gene activation. Conversely, heterochromatic mouse satellites sediment faster than bulk chromatin, suggesting that they are packaged into especially compact and regular fibers (Gilbert and Allan, 2001). However, to understand the global relationships between chromatin fiber structures, genes, and gene expression, chromatin fiber structure needs to be investigated at a genomic level.

We have analyzed the distribution of compact and open chromatin fibers across the human genome by hybridization to metaphase chromosomes and to genomic microarrays. We conclude that human heterochromatin is surprisingly heterogeneous in structure and that there is not a simple structural division between heterochromatin and euchromatin. Most human satellite DNAs (especially α-satellite and satellite 2) are packaged in compact chromatin fibers and are absent from open fiber fractions, but some satellite 3 is in open chromatin fibers. Some regions of euchromatin (G-bands) are also enriched in compact fibers.

In contrast, we show that open chromatin fibers originate from the most gene-rich regions (T-bands) of the human genome (Holmquist, 1992; Craig and Bickmore, 1994). Surprisingly there is not a simple correlation between gene expression and open chromatin fibers. Many transcriptionally inactive genes are in open chromatin fiber domains. Conversely, in regions of low gene density, active genes can reside within large domains of

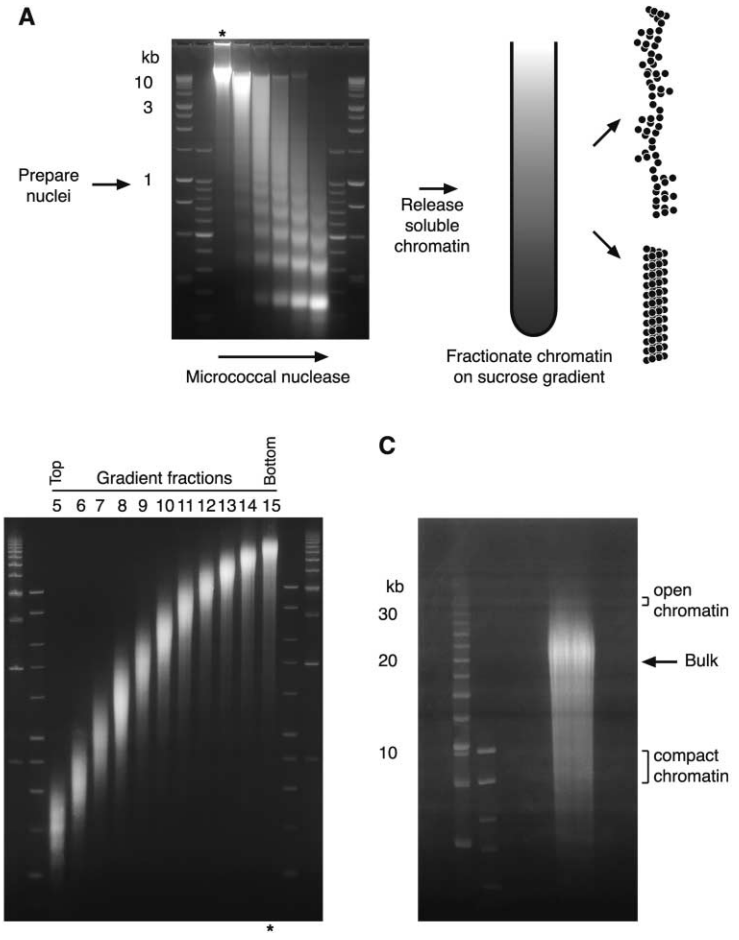

Figure 1. Sucrose Gradient Fractionation of Human Chromatin

(A) MNase digestion of nuclei was used to produce chromatin fragments with a size of ~20 kb. The soluble chromatin from the digest marked by an asterisk, was run on a 6–40% isokinetic sucrose gradient. For two chromatin fragments of equal length (kb) the more open/disordered fragment (top) will sediment slower than the more compact/rigid one (bottom)

(B) The gradient was fractionated from top to bottom and the DNA purified from each fraction examined by agarose gel electrophoresis.

(C) To isolate DNA fragments from the same fraction (sedimentation rate), but with different lengths (and thus different chromatin fiber conformations), DNA from a gradient fraction (asterisked in B) was size selected by PFGE. DNA was purified from a gel slice corresponding to the peak of EtBr staining (bulk chromatin). To represent "compact" chromatin, DNA was purified from a gel slice containing fragments ~10 kb shorter than the EtBr peak. DNA from "open" chromatin was purified from a gel slice containing fragments ~10 kb longer than bulk chromatin.

compact fibers. We show that there is a link between the structure of the chromatin fiber and higher-order levels of chromatin condensation in the nucleus. Chromosomal domains that are enriched in open fibers are also decondensed cytologically, and they locate outside of chromosome territories.

It has been suggested that the clustering of genes together in the human genome reflects an impact of some higher-order level of chromatin structure on gene expression (Caron et al., 2001; Lercher et al., 2002; Versteeg et al., 2003). We suggest that open chromatin fiber domains may create a chromatin landscape that facilitates transcriptional activation when the correct transcription factors are present. This could impose a constraint to maintain clusters of genes together in the genome during evolution.

Results

Sucrose Gradient Sedimentation of Chromatin Fibers from the Human Genome

Chromatin fiber structures can be separated by sucrose gradient sedimentation (Kimura et al., 1983; Fisher and Felsenfeld, 1986; Gilbert and Allan, 2001; Kim and Clark, 2002). Sedimentation rate is determined by the mass (DNA length and protein composition), and hydrodynamic shape (conformation) of the fiber. A given length of DNA will sediment faster than bulk chromatin if it is packaged into a more compact regular chromatin structure (Gilbert and Allan, 2001), and slower if it is packaged in fibers whose structure is interrupted by discontinuities that increase the frictional coefficient (Kimura et al., 1983; Fisher and Felsenfeld, 1986; Caplan et al., 1987) (Figure 1A).

To investigate human chromatin fiber structure we digested nuclei from lymphoblastoid cells with micrococcal nuclease (MNase), which cuts chromatin in the linker between nucleosomes. In the solenoid model of the 30 nm fiber, there are six nucleosomes per helical turn (~1.2 kb) (Thoma et al., 1979; McGhee et al., 1983; Wolffe, 1998), so to analyze structure that is propagated over extensive regions (50–150 nucleosomes), we used digestion conditions which gave fragments of 10–30 kb average length (Figure 1A). Transcriptionally active regions are commonly considered to be more sensitive to nuclease digestion than inactive regions, but this is generally seen with DNaseI not MNase (Weintraub and Groudine, 1976; Bellard et al., 1978; Sun et al., 2001). To ensure that we were not preferentially releasing particular parts of the genome before loading onto the gradient, total genomic DNA and DNA from the digested soluble (input) chromatin were hybridized by fluorescence in situ hybridization (FISH) to metaphase chromosomes. In the presence of suppression of repeat hybridization by human CotI DNA, input chromatin and total genomic DNA hybridization signals along the euchro-

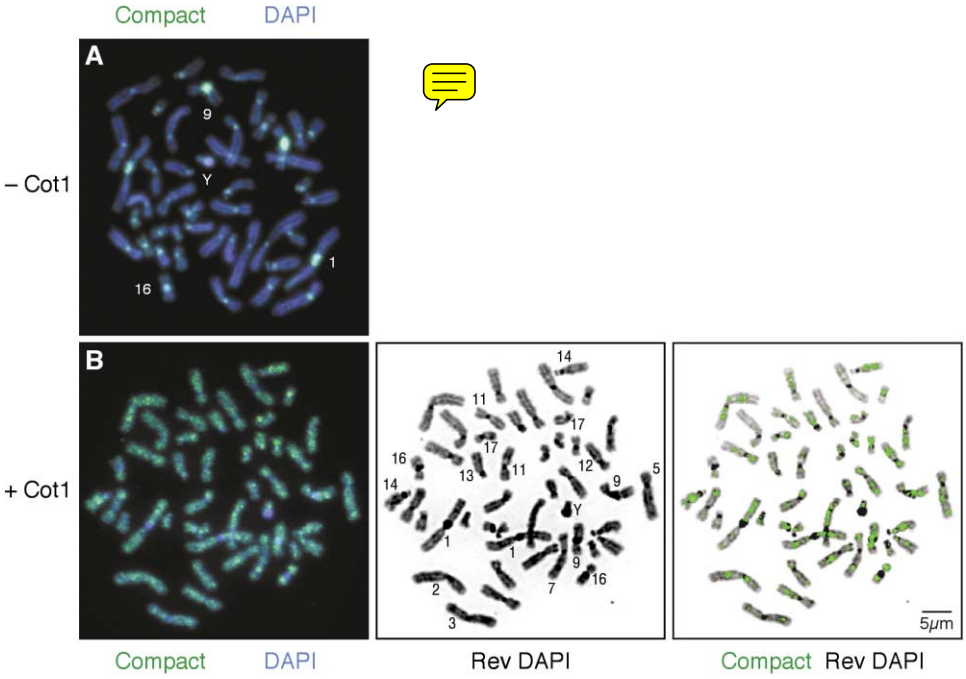

Figure 2. Compact Human Chromatin Fibers Originate from Heterochromatin and a Subset of G-Bands

FISH to human metaphase chromosomes with blunt-end linkered "compact" chromatin.

(A) In the absence of suppression by human CotI, hybridization (green) is predominantly to centromeres and the juxtacentromeric heterochromatin at 1q12, and 9q12. Note the absence of hybridization to the heterochromatin at 16q11 and Yq.

(B) After Cot1 suppression, hybridization (green) on the chromosome arms is to G-bands. The reversed DAPI signal was used to identify the chromosomes (middle image), and the strongest (thresholded) sites of hybridization were superimposed on the banded chromosomes (right image).

matic part of chromosome arms were indistinguishable (Supplemental Figure S1 available at http://www.cell.com/cgi/content/full/118/5/555/DC1). Without CotI suppression, biotin-dUTP labeled genomic DNA and input chromatin both hybridize strongly to centromeric and juxtacentromeric heterochromatin, showing that it is not refractory to digestion and solubilization (Supplemental Figures S1A and S1B available on *Cell* website). Probes labeled with biotin-dCTP detect these satellites poorly because of their AT-richness (60%) (Tagarro et al., 1994) (Supplemental Figure S1C available on *Cell* website). Therefore, all subsequent FISH data are from DNAs labeled with dUTP.

Digested chromatin was sedimented through an isokinetic sucrose gradient (6%–40%) (Noll and Noll, 1989). The gradient was fractionated from top to bottom so that fractions contain chromatin fibers with progressively increased sedimentation rate. Each fraction will contain fibers of the same sedimentation rate, but will consist of both DNA fragments of equal length with the same chromatin structure/compaction, as well as shorter and longer fragments in more rigid/compact, or more disordered/open chromatin fibers, respectively. To separate these we resolved the DNA fragments from a fraction according to their size, by agarose gel electrophoresis (Figure 1B). The peak of ethidium bromide (EtBr) staining corresponds to sequences that were packaged within fibers characteristic of the bulk genome. However, in each fraction there are smears of DNA fragments that are shorter or longer than those in the EtBr peak, and these should respectively contain sequences packaged in fibers that are more, or less, compact than those of the bulk genome (Figure 1C).

Some Human Satellites Are Packaged into Compact Chromatin Fibers

Mouse major and minor satellites are packaged into 30 nm fibers that are more compact and regularly folded than those of bulk chromatin (Gilbert and Allan, 2001). The human genome contains a complex set of satellite repeats. α-satellite is present at each centromere, blocks of satellites 1, 2, and 3 and the β-satellite are present in juxtacentromeric blocks of heterochromatin (Tagarro et al., 1994; Shiels et al., 1997). To identify regions of the human genome that are packaged into the most compact chromatin fibers, we isolated DNA fragments from a sucrose gradient fraction that were 5–10 kb shorter than those of the EtBr peak (Figure 1C). This DNA was hybridized to metaphase chromosome spreads (Figure 2). Without CotI suppression most hybridization signal was at sites of constitutive heterochromatin (C-bands), each of the centromeres, and juxta-centromeric heterochromatin at 1q12 and 9q12. Hybridization to C-bands at 16q11 and Yq was less apparent (Figure 2A). Therefore some, but not all, human satellite repeats are enriched in compact chromatin fibers.

In the presence of excess CotI, to suppress repetitive sequences, hybridization signal from the compact chromatin fraction was enriched in some euchromatic re-

gions (Figure 2B). Many of these sites (e.g., 1p31, 1q31, and q41; 3p24 and q24; 5q34, 7p21, and q21; 9q31, 12q21, 16p12) corresponded with intensely staining G-bands that are depleted of genes (Furey and Haussler, 2003; http://www.ensembl.org/Homo_sapiens/). Hence, euchromatic regions of the human genome with a very low gene density appear to be packaged in chromatin fibers with a similar level of compaction to heterochromatin.

Gene-Dense Regions Are Enriched in Open Chromatin Fibers

To identify what sequences are enriched in slowly sedimenting ("open") chromatin fibers, DNA was purified from the EtBr peak of a gradient fraction to represent bulk chromatin structure, and from the smear of fragments that are ~10kb longer than this (open chromatin) (Figure 1C). Cohybridizing bulk (red) and open (green) fractions to metaphase chromosomes did not give a uniform yellow signal, as would be expected if these chromatin structures were interspersed throughout the genome. Instead, distinct regions of the karyotype were enriched in open chromatin, and so appear greener (Figure 3A). The most gene-rich human chromosomes (HSA) are HSA16, 17, 19, and 22 (Craig and Bickmore, 1994; Venter et al., 2001) and these all hybridize strongly to open chromatin (Figure 3B). In contrast, gene-poor HSA4, 13, and 18 hybridize poorly.

At a subchromosome level, gene-rich T-bands (Holmquist, 1992; Craig and Bickmore, 1994), for example at the distal end of 1p (1p34-p36), and at 11q13 and q23, are enriched in open chromatin (Figures 3B and 4A). These regions also contain abundant Alu repeats (Holmquist, 1992) but their detection is suppressed by CotI. Since sites of hybridization to open chromatin fibers, e.g., 7q11.2 and q22 and q36 in Figure 3C, are not suppressed even by very large amounts of CotI, we are detecting single (or low) copy sequences in the open chromatin fraction. We conclude that regions of highest gene density have a more open chromatin fiber conformation than the rest of the human genome.

Without CotI, there was strong hybridization of open chromatin to gene- and Alu-rich parts of the genome (e.g., 9q34, in Figure 3D) as expected, but no hybridization to centromeric α-satellite (Figures 3C and 3D) or satellite 2 at 1q12 (data not shown). This suggests that no part of these heterochromatic regions is packaged into open chromatin fibers. However, there was strong hybridization to the satellite 3 at 9q12 (Tagarro et al., 1994) (Figure 3D). This C-band also hybridizes to compact chromatin (Figure 2) and so, despite its apparently simple sequence composition, it appears to have a heterogeneous chromatin fiber structure.

Analysis of Open Chromatin Fibers Using Genomic Microarrays

FISH gives an immediate visual impression of the gross distribution of open chromatin fibers in the human genome, but is limited by the resolution of chromosomes bands (~5–10Mb). To analyze the distribution of open chromatin at higher resolution, and to relate it directly to the genome sequence, we cohybridized differentially labeled "open" and input chromatin fractions to a genomic DNA microarray. The array was assembled from clones, spaced at ~1 Mb intervals, from the "golden path" used in the sequencing of the human genome (Fiegler et al., 2003). Self:self hybridizations (Cy3 input chromatin versus Cy5 input, and Cy3 bulk chromatin versus Cy5 bulk) gave mean hybridization ratios of 1.003 (s.d = 0.051) and 0.998 (s.d. = 0.031) respectively, confirming the consistency of hybridization and the absence of random scatter. Likewise, hybridization of total (female) genomic DNA:(male) input chromatin also gave an average hybridization ratio close to 1 for each autosome suggesting that there is no preferential release of chromatin from, for example, gene-rich domains (Supplemental Table S1 available on *Cell* website), consistent with FISH results (Supplemental Figure S1 available on *Cell* website).

Two separate isolations of open chromatin were each hybridized twice versus input chromatin, using color reversal. There was a strong correlation between the results of replicate hybridizations performed with color reversal (Supplemental Figures S2 and S3 available on *Cell* website). Because only small amounts of open chromatin fraction could be prepared for labeling compared with the amounts of input control, we are only able to give comparative, not absolute, levels of its enrichment across the genome. Domains of the human genome enriched in open chromatin ($\log_2$ ratio > 0) (Supplemental Figure S4 available on *Cell* website) correspond with the results obtained by FISH. Chromosomes with the highest overall ratio of open:input chromatin are the gene-rich HSA17, 19 and 22 which also hybridized strongly to open chromatin by FISH (Figure 3). The autosomes most depleted in open chromatin fibers are gene-poor HSA4 and 13 (Supplemental Table S1 available on *Cell* website). The correlation between enrichment of open chromatin and gene density was quantified by linear regression ($r^2 = 0.88$) (Figure 5).

FISH and microarray data also correspond at chromosome band level. For example, there is enriched open chromatin at clusters of BACs at the distal end of 1p (1p34-p36; 0–45 Mb), and at 1q21 (144–153 Mb), regions that also hybridize strongly to open chromatin by FISH (Figure 4A). Likewise the major domains of FISH signal from open chromatin on HSA11 at 11p15, 11q13, and 11q23-q25, correspond with peaks of hybridization on the microarray (0–20 Mb, 63–76 Mb and 110–134 Mb) (Figure 4A). However, microarray analysis affords higher resolution analysis than FISH. For example, by FISH open chromatin appears to hybridize to almost all of 16p, whereas there are peaks and troughs in the microarray hybridization pattern (Figure 4A). To analyze this in more detail, we examined the distal part of 16p BAC by BAC. BACs in distal 16p13.3 (0–1 Mb) and the proximal part of this band (3.5–5.5 Mb) show an enrichment of open chromatin fibers in replicate experiments (Figure 4B). Open chromatin fibers are depleted in the intervening region (2 Mb), and also in the adjacent chromosome band 16p13.2 (8–10 Mb). Enrichment of open chromatin then recurs in 16p13.1 (10.5 Mb). This mirrors the transition between chromosome bands 16p13.3-p13.1, and the gene density profile of 16p (Figure 4B).

To analyze open chromatin distribution at even higher resolution, and on contiguous sequence, we hybridized it to a chromosome 22q array consisting of overlapping sequencing tiling path clones (Woodfine et al., 2004).

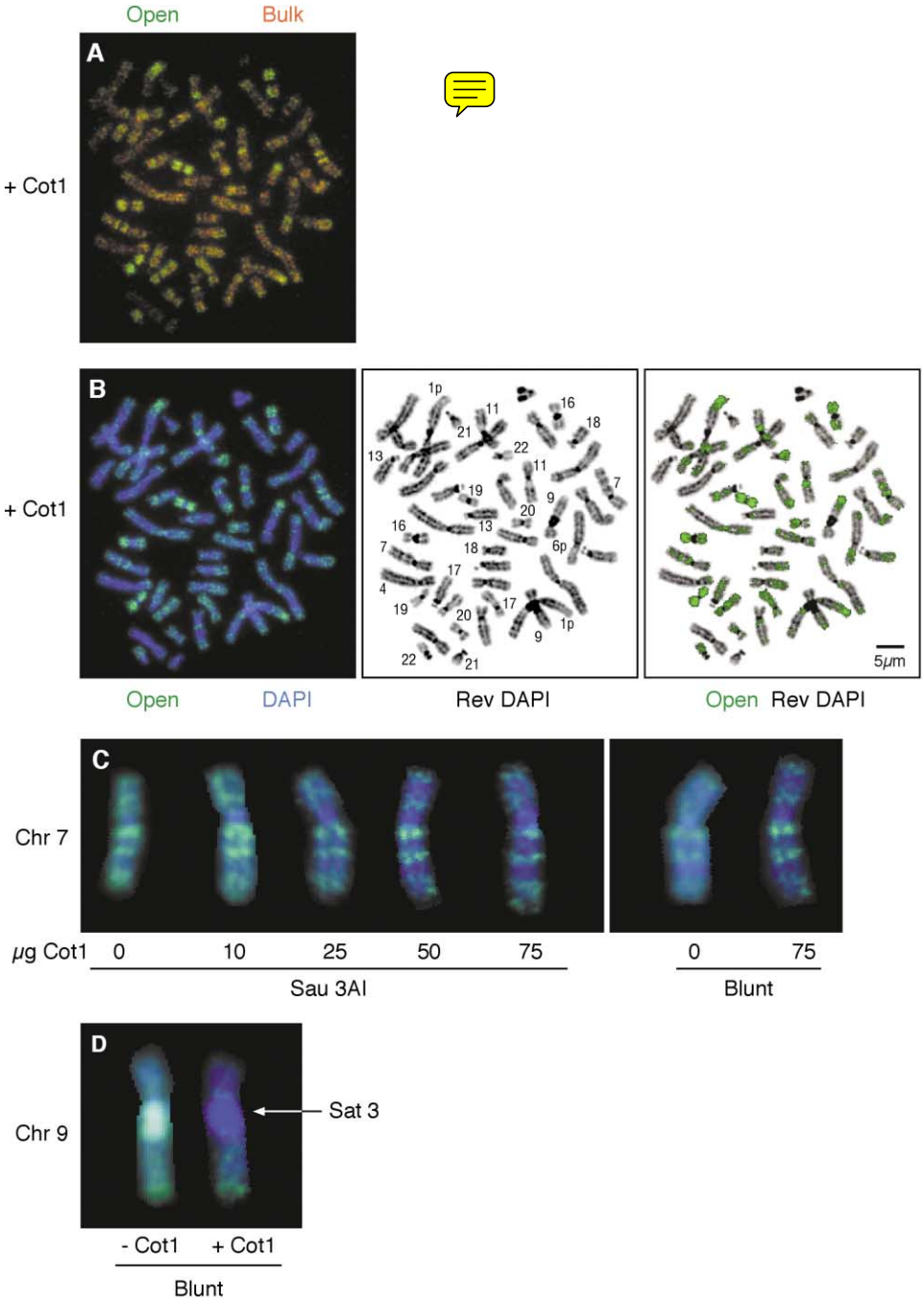

Figure 3. Open Human Chromatin Fibers Hybridize to the Most Gene-Dense Parts of the Genome

(A) FISH onto metaphase chromosomes, with Sau3AI linkered "bulk" biotin-labeled (red) and "open" digoxigenin-labeled (green) chromatin probes, in the presence of suppression with 50μg Cot1.

(B) Hybridization signal from "open" chromatin on DAPI stained (blue) chromosomes (left image). The reverse DAPI signal was used to identify the chromosomes (middle image) and the strongest (thresholded) sites of open chromatin hybridization (green) are superimposed on the banded chromosomes (right image).

(C) HSA7 hybridized with open chromatin fraction, either Sau3A1 or blunt-end linkered, in the presence of increasing amounts of human CotI DNA.

(D) HSA9 hybridized with blunt-ended open chromatin fraction in the absence or presence of 50μg of CotI DNA. When the compact chromatin fraction was digested with Sau3A1 prior to linker-ligation the 9q satellite was not detected since it lacks Sau3AI recognition sites (data not shown).

The average resolution of this array is 78 kb but it contains regions where the clones are even smaller than the size of the chromatin fibers being examined. There is a strong correspondence between the open:input hybridization ratio and gene density. On this generally gene-rich chromosome arm, domains depleted of open

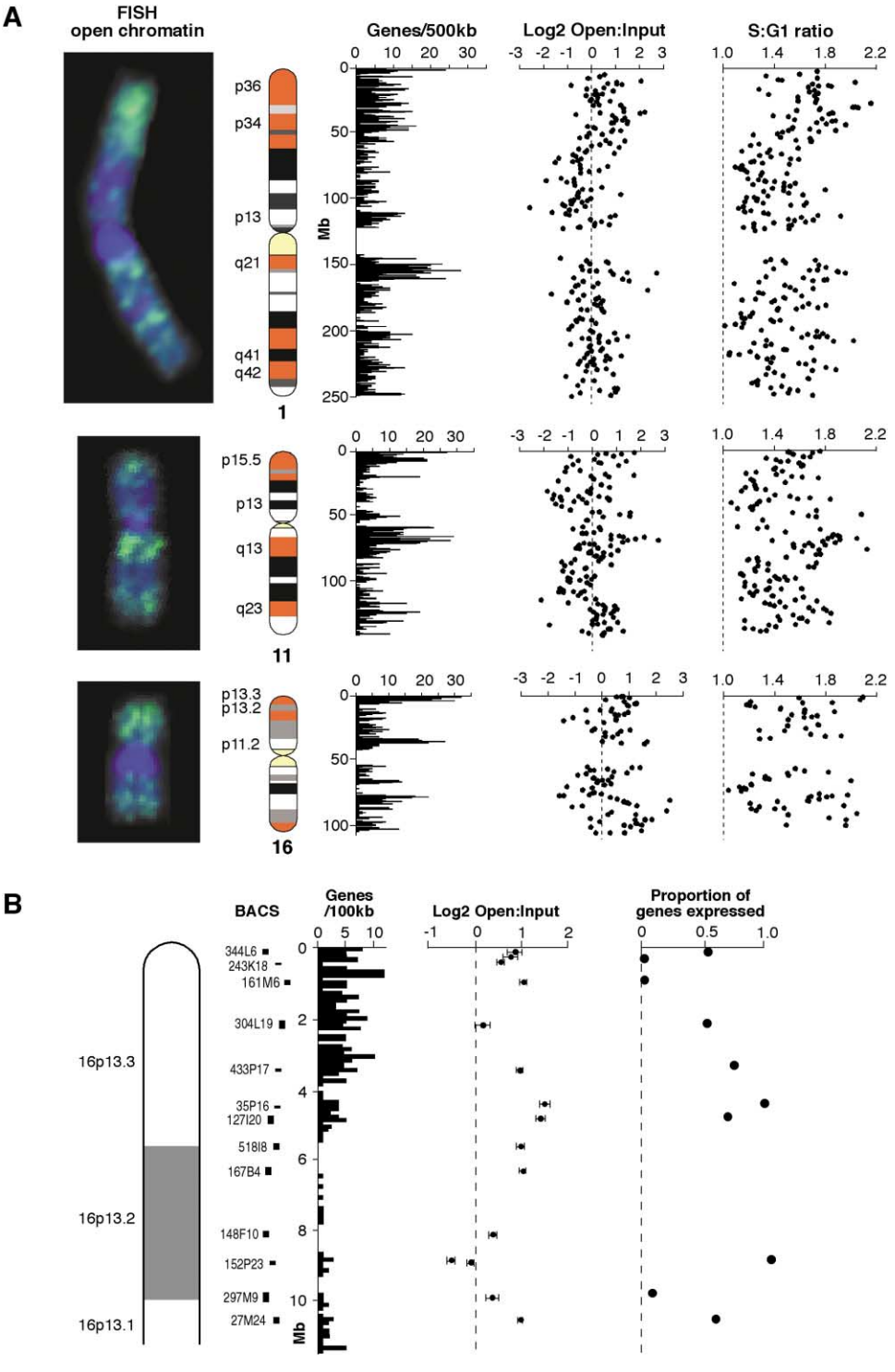

Figure 4. Comparing FISH and Microarray Analysis of Open Chromatin

Sau3AI linker-ligated open chromatin fraction was hybridized to a whole genome 1 Mb microarray using an input chromatin control. (A) Log2 open:input hybridization ratios for HSA1, 11 and 16 are shown aligned with chromosomes hybridized with open chromatin by FISH and with ideograms of the chromosomes with T-bands highlighted in red. The gene density for Ensembl genes is shown for a 500 kb window. Replication timing (S:G1 ratio) of these chromosomes, established using the same 1 Mb genomic array, is also shown (Woodfine et al., 2004). (B) Mean log2 ratio (±S.E.M. for 4 replicate experiments) of open:input hybridization signal for individual BACs from 16p13 aligned to the DNA sequence (Mb), gene density/100 kb window, and the proportion of expressed genes in each BAC.

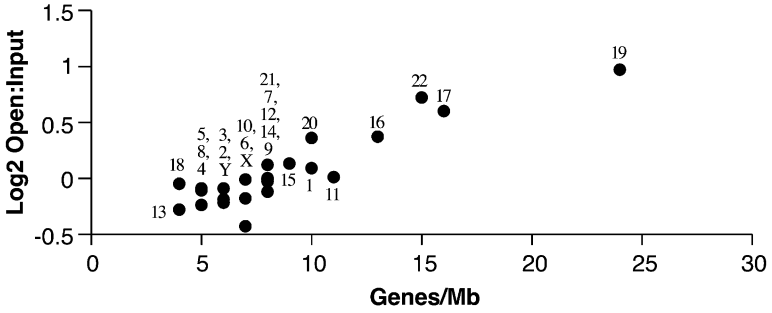

Figure 5. Correlation between the Abundance of Open Chromatin Fibers and Gene Density

Linear regression analysis between the gene density (Ensembl genes/Mb) and the mean log2 of open: input chromatin per chromosome (averaged between two independent hybridizations to the 1 Mb array, and performed with color reversal). Chromosome number is indicated next to each data point. $r^2 = 0.88$.

chromatin fibers correspond with the gene-poor regions of 22q12.1 (26–27.3 Mb), q12.3 (30.7–32.2 Mb), and q13.31-q13.32 (45.5–47.4 Mb) (Figure 6A). Clones with enriched hybridization to open chromatin tended to be clustered in contiguous regions, as did clones depleted of open chromatin (variance in log2 value across the whole array = 0.4, average variance between log2 of a clone and that of its flanking contiguous clones = 0.28). Transitions between regions of open and closed chromatin fiber structure are generally sharp, not gradual, suggesting that there may be distinct boundaries between them.

Correlations of Open Chromatin Structure to Replication and Gene Expression

Replication timing in lymphoblastoids has also been analyzed on the 1 Mb whole genome and 22q high resolution arrays (Woodfine et al., 2004). There is a good correlation between the presence of open chromatin fibers and early replication at 1 Mb resolution ($r^2 = 0.85$) (Supplemental Table S1 available on *Cell* website). However, there are also places where replication time and chromatin fiber structure differ. These are generally telomeric regions. Many telomeric regions are gene-rich T-bands and are both early replicating and in open chromatin fibers. However some chromosome ends do not correspond with T-bands, are not enriched in open chromatin fibers, yet are early replicating (e.g., 18qter) (Supplemental Figure S4 available on *Cell* website). Conversely, 6qter is a late replicating region that is enriched in open chromatin. The correlation between chromatin structure and replication timing also breaks down when analyzed at high resolution on 22q ($r^2 = 0.05$) (Figure 6A). In general, the regions of 22q most enriched in open chromatin fibers are also early replicating, but there are many places that are depleted of open chromatin but still replicate early. This suggests that replication timing and 30 nm chromatin fiber are not functionally linked.

Gene-rich regions also generally have a high GC base composition (Saccone et al., 1993), and so not surprisingly there is also a correlation between open chromatin fiber structure and base composition at the whole genome level ($r^2 = 0.94$) (Supplemental Table S1 available on *Cell* website). However, Woodfine et al. (2004) noticed that in distal 22q (43–47 Mb) there is a GC-rich R-band that is an unusually gene-poor region. This region is generally depleted of open chromatin and is late replicating (Figure 6).

Is the correlation between the presence of open chromatin fibers in the human genome and gene density simply due to gene expression? The gene expression profile of lymphoblasts has been determined on a gene expression microarray (Woodfine et al., 2004). There is not a simple relationship between gene expression and enrichment of open chromatin fibers. At a whole chromosome level, there is no correlation between the chromosome average open:input hybridization ratio and either the average expression level ($r^2 = 0.06$), or the probability of expression ($r^2 < 0.01$) of genes assayed on each chromosome (Supplemental Table S1 available on *Cell* website). There is also no correlation between the probability of gene expression, or the gene expression level, at an individual BAC level in the 1 Mb or the high resolution 22q array analyses (Figures 4B and 6A). To examine chromatin fiber structure at individual genes, we identified contiguous high-resolution clones in 22q11.21 and q12.1. 22q11.21 is gene rich and in the 500 kb region analyzed (17.8–18.3 Mb), we identified 8 genes, but only one of them (*UFD1L*) is transcriptionally active. Nevertheless, most of the region, including the inactive genes, is enriched in open chromatin fibers. The region depleted of open chromatin at 17.90–18.05 Mb corresponds to an intergenic region (Figure 6B). Therefore, we conclude that it is not transcription per se which is opening the chromatin fiber. Conversely, 22q12.1 is gene poor but in the middle of a 1.4 Mb region examined (26.0–27.4 Mb) there is a small cluster of three genes and one of them (*PITPNB*) is transcriptionally active. However, the entire region is depleted of open chromatin fibers (log2 open:input < 0) (Figure 6C). Therefore, transcription of an individual gene can still occur within the context of a broad domain of compact chromatin fibers.

Open Chromatin Fiber Domains Are Cytologically Decondensed and Locate Outside of Chromosome Territories

A slowed chromatin fiber sedimentation rate could result from reduced mass (loss of protein), but is unlikely. To account for the difference in sedimentation rate between open and bulk chromatin, we calculate that an open fiber would have to lose either 76 kDa of protein per nucleosome, or 2/3 of the nucleosomes themselves. Therefore, we argue that slowed sedimentation is due to a change in the shape and structure of the "open" fibers, which increases their frictional coefficient. An inactive repetitive fragment of the chicken genome has been shown to have hydrodynamic properties consistent with a rod-like particle (Ghirlando et al., 2004), and the structure of mouse satellite-containing chromatin has been interpreted as more regularly folded 30 nm

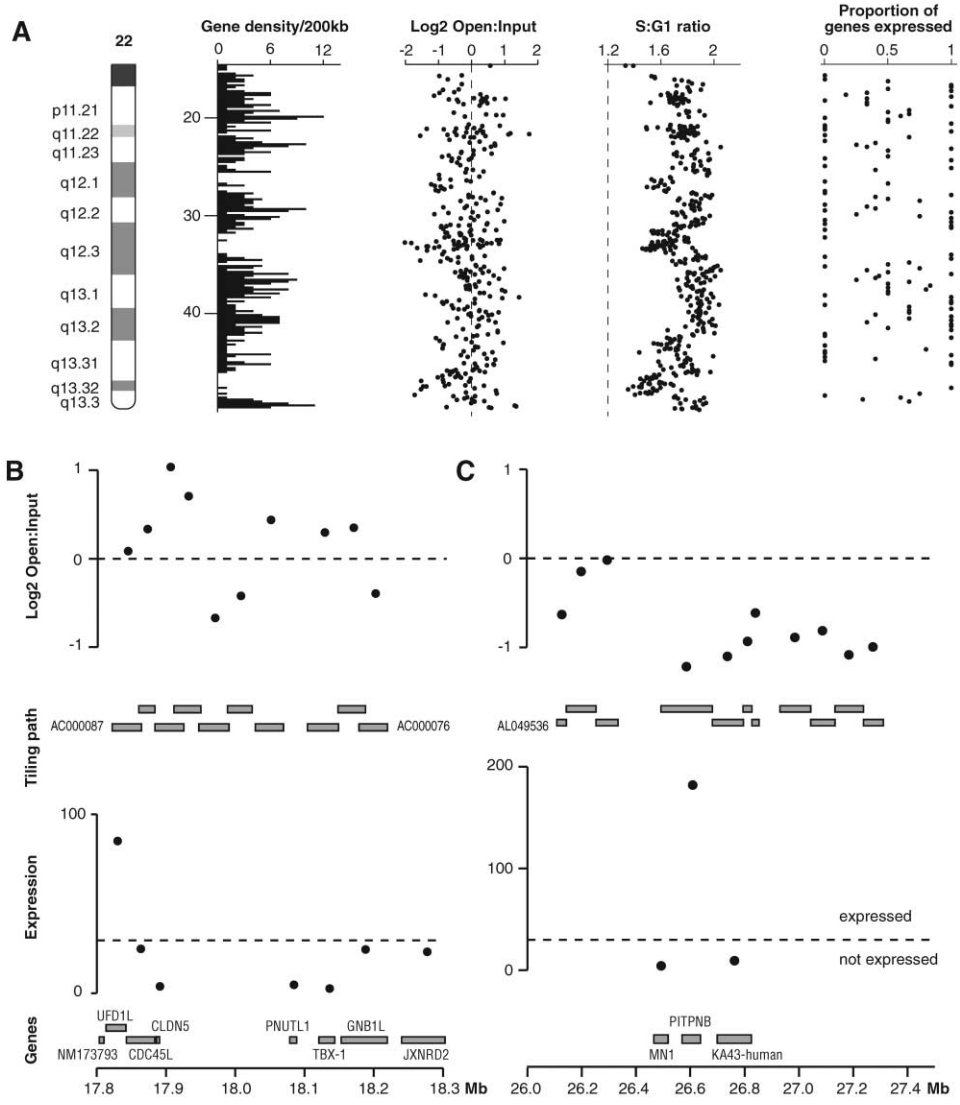

Figure 6. High Resolution Analysis of Open Chromatin on 22q

(A) Sau3AI linker-ligated open chromatin fraction was hybridized to a high-resolution contiguous tiling path array of 22q. Log2 ratio of open:input hybridization signal for each clone aligned to the DNA sequence (Mb), gene density/200 kb window, and the replication timing S:G1 for this array (Woodfine et al., 2004). The proportion of genes expressed in a 200 kb window is also shown. The log2 open: input chromatin, tile path, genes, and their expression level are aligned for; (B) 500 kb of 22q11.21; (C) 1.4 Mb of 22q12.1. The cut off point to determine whether a gene is expressed or not was set as 30 (Woodfine et al., 2004).

fibers, with less discontinuities, than bulk chromatin (Gilbert and Allan, 2001). Therefore the "open" human chromatin fibers that we identify here could be packaged into 30 nm chromatin fibers peppered with frequent or large deformations.

Could open 30 nm fiber structure be transmitted through to higher-order chromatin and nuclear structure? There is a linear relationship between the mean-square interphase separations (d^2) of FISH probe signals and their genomic separation (kb) (van den Engh et al., 1992). This has been used to show that regions of the human genome can have different levels of higher-order chromatin compaction (Yokota et al., 1997). To determine if regions enriched in open chromatin fibers are also cytologically more decondensed than regions on the same chromosome that are depleted of "open" chromatin, we analyzed the interphase distances between probes for two regions of 11p in lymphoblast nuclei. In distal 11p15.5 (1–2.5 Mb), all BACS analyzed are enriched in open chromatin fibers (log2 $>$ 0). Further down the chromosome arm (11p14.1-p13; 27.5–32.0 Mb), all BACs assayed are depleted of open chromatin (Figure 7A). For both regions, there is a linear relationship between d^2 and genomic separations of 0.25–2.0 Mb (Figure 7B). However, the slopes of the lines indicate that 11p15.5 is less cytologically condensed ($d^2 = 1.1 \mu m^2$/Mb) than 11p14.1-p13 ($d^2 = 0.30\ \mu m^2$/Mb) (Figure 7B). We conclude that regions of open chromatin fibers exist in a physically decondensed higher-order state in the nucleus.

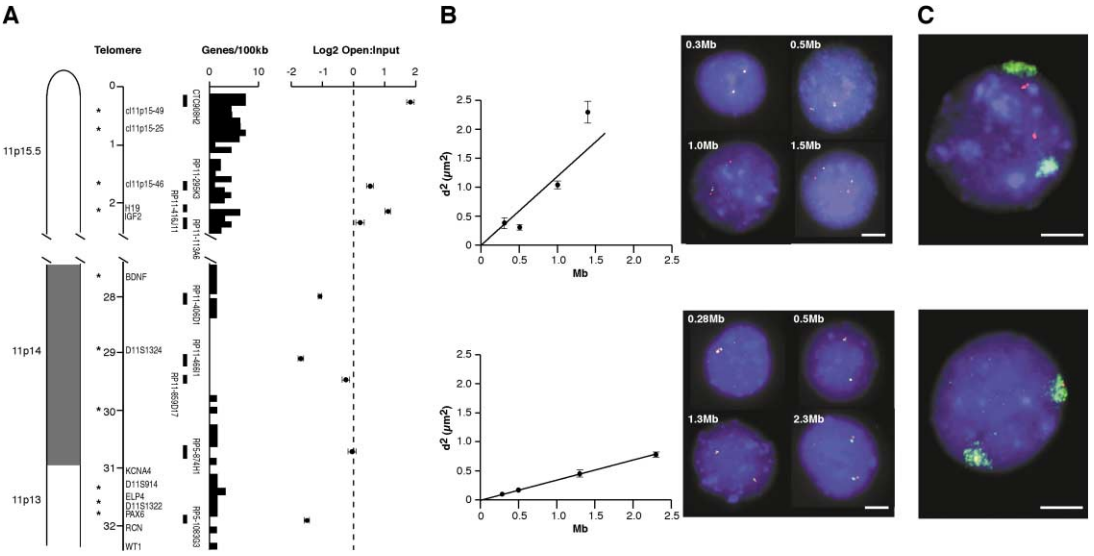

Figure 7. Chromatin Fiber Structure, Chromatin Condensation, and Nuclear Organization of 11p

(A) Average log2 open: input chromatin ratio for BACs in 11p15.5, and p14.1-p13, aligned to DNA sequence (Mb) and gene density/100 kb window.

(B) Graphs of mean square interphase distance (d^2 in μm^2) ($\pm$SEM) between FISH signals for pairs of probes (asterisked in A) from 11p15.5 (top) and p14.1-p13 (bottom) (n = 50). Representative images for probe pairs (red and green) at different Mb separations are shown to the right of each graph. DNA is counterstained with DAPI (blue).

(C) Representative FISH images for individual probes (red) and the 11p territory (green) for (top image) an 11p15.5 probe (cI11p15-25) and (bottom image) *PAX6* in 11p13. For 11p15.5, the probes (red) often (80%) localized outside the chromosome territory (green); while for 11p14.1/11p13, the probes were normally (89%) located inside the territory. Nuclei are counterstained using DAPI. Scale bar is equal to 5 μm.

Probes from regions of high gene density have previously been shown to have a distinctive nuclear organization—they locate outside of chromosome territories. All of the regions that have so far been identified outside of chromosome territories in lymphoblastoid cells correspond with regions of open chromatin fibers. These include; the MHC class II at 6p21.3 (32.6–33.4 Mb) (Volpi et al., 2000), 11p15.5 (0–2 Mb) (Figure 7C), 11q13, and distal 16p13 (0.17–0.2 Mb) (Mahy et al., 2002). In comparison, probes from the more cytologically condensed region of 11p13-p14 locate inside of the 11p territory (Figure 7C). There is also a correspondence between the regions that are known to locate outside of the 22q territory (Mahy et al., 2002) and our high-resolution analysis of open chromatin fibers (data not shown). Therefore the structure of the 30 nm fiber may even affect this level of nuclear organization.

Discussion

Chromatin Fiber Structures at Heterochromatin

Even though heterochromatin appears cytologically compact (C-bands), biophysical evidence for a compact chromatin structure is limited. Mouse major and minor satellites have been shown to have a compact fiber structure (Gilbert and Allan, 2001). Here, we show that human centromeric α-satellites and the juxtacentromeric satellite 2 and 3 on HSA 1 and 9 are enriched in compact chromatin fibers (Figure 2A). However, there is more heterogeneity in the fiber structure of human heterochromatin than in the mouse. Neither 16q11, nor the large block of heterochromatin at Yq12, hybridize well to compact chromatin (Figure 2A). We were also surprised to find that 9q12 hybridizes strongly to open chromatin (Figure 3D), suggesting that the structure of satellite 3 is different from that of α-satellite and satellite 2. It has recently been shown that transcription of satellite 3 from 9q12 can be induced by heat shock (Jolly et al., 2003; Rizzi et al., 2004), so this region may be in a transcriptionally poised state. We conclude that human heterochromatin is comprised mainly of compact chromatin fibers, but that it should not be considered as a uniform structure.

Some G-bands are also enriched in compact chromatin fibers (Figure 2B), and depleted of open ones (Supplemental Figure S4 available on *Cell* website). This suggests that some gene-poor euchromatin may be in chromatin fibers of similar structure (sedimentation rate) to those from constitutive heterochromatin. Therefore, there may not be a simple structural distinction between "heterochromatin" and "euchromatin" at the level of the 30 nm chromatin fiber.

Open Chromatin Fibers Originate from Gene-Rich, but Not Necessarily Transcriptionally Active, Regions of the Human Genome

We have shown that the fraction of the human genome with a very "open" chromatin structure originates from the most gene-rich domains (Figures 3–6 and Supplemental Figure S4 available on *Cell* website). High-resolution analysis on 22q indicates that the regions of open chromatin fiber structure are generally contiguous over $>$100 kb and extend over several genes (Figure 6). The generally sharp transitions between "open" and "closed" chromatin suggest that there may be distinct boundaries between these two chromatin structures.

The only previous analysis of chromatin fiber structure for vertebrate genes was at the chicken globin and ovalbumin loci (Kimura et al., 1983; Fisher and Felsenfeld, 1986; Caplan et al., 1987). From these studies, it might have been assumed that open chromatin fiber structure would correlate with gene expression. However, we have found that the packaging of gene-dense regions in open chromatin fibers is not simply a reflection of transcription from these regions. At a whole chromosome level, there is no correlation between the abundance of open fibers and either the average levels of gene expression for that chromosome in lymphoblasts, or the probability of gene expression (Woodfine et al., 2004) (Supplemental Table S1 available on *Cell* website). At high resolution on 22q, we found gene-rich, but transcriptionally inactive, regions that are nonetheless enriched in open chromatin fibers. Conversely, an active gene within a gene-poor area was in a large domain depleted of open chromatin fiber structure. This latter observation does not preclude that there may be a localized alteration of chromatin structure at this gene, that does not affect the level of 30 nm fiber structure being analyzed here. We conclude that domains of open chromatin fibers may mark out regions that have the potential for transcription, given the right transcription factor environment. In this regard it is of interest to note that, in yeast, chromatin-remodeling events that lead to the formation of slowly sedimenting chromatin fibers are also independent of transcription itself (Kim and Clark. 2002).

Relating Chromatin Fiber Structure to Nuclear Organization

We do not know the precise structure or cause of open chromatin fibers, for example whether they might be attributable to DNase I hypersensitive sites disrupting the continuity of the fiber, but they seem to impact on the ability to form higher-order structures. We have shown that a region of the human genome (11p15.5) enriched in open chromatin fibers is cytologically 2-fold less compact than a region from the same chromosome (11p13-14) that is depleted of open fibers (Figure 7). This is consistent with the overall more decondensed nuclear structure of HSA19 compared with that of HSA18 (Croft et al., 1999) (Figure 5 and Supplemental Table S1 available on *Cell* website).

Volpi et al. (2000) suggested localization outside of chromosome territories may be a visual manifestation of an open or decondensed chromatin structure propagated over long stretches of chromatin. Our data are certainly consistent with this idea. However, the decondensed regions must still retain higher-order structure beyond the 30 nm fiber. Upon induction, the murine *HoxB* loci decondenses cytologically, and loops out from its chromosome territory, to an extent consistent with unwinding to a 30 nm chromatin fiber ($d^2 = 0.88$ μm^2 for a 90 kb region) (Chambeyron and Bickmore, 2004). However, the cytological compaction level at 11p15.5 in lymphoblastoid cells is 10-fold higher than this ($d^2 = 1.1$ μm^2/Mb) (Figure 7B). Opening of 30 nm chromatin fiber structure might be necessary for the transcriptional potential of a region, and to allow for subsequent chromatin decondensation events that accompany the induction of high levels of transcription.

Chromatin Structure, Genome Evolution, and Plasticity

The availability of the human genome sequence has led others to examine whether gene distribution is random or subject to evolutionary selection. It has been suggested that domains of high levels of transcription represent a higher-order structure in the human genome (Caron et al., 2001; Versteeg et al., 2003) that results from the impact of chromatin structure on transcription rate. However, Lercher et al. (2002) found a similarity in the breadth of expression across different cell types, and not the level of transcription, for genes that are clustered together. They suggested that selection is therefore acting to favor the clustering of widely expressed (housekeeping) genes in a chromatin structure that remains in an open configuration in many cell types. Our demonstration that open chromatin fibers are generally enriched in gene-rich domains, and not just those regions that are transcriptionally active, is consistent with this latter idea. We propose that an open/disordered 30 nm chromatin fiber structure creates an environment that facilitates transcription and so can act to maintain clusters of widely expressed genes together in these regions during evolution. Evidence to support this idea comes from an analysis of the 8 breaks in synteny between HSA22q and the mouse genome (http://www.ensembl.org/Homo_sapiens/mapview?chr=22). None of the synteny breaks disrupts a region of contiguous open chromatin fibers.

Since gene-dense regions are also enriched in SINE repeats (Venter et al., 2001; Versteeg et al., 2003), there may be a preference for these retroposons to integrate into regions of open fibers. Recently preferential genomic sites of HIV integration were reported (Schroder et al., 2002). Analysis of these sites (e.g., 6p21.3, 11q13, 19) shows that they correspond well with the domains of open chromatin fibers that we describe here. Therefore, the integration pattern of this retrovirus into the human genome might be influenced by chromatin fiber structure.

We have provided a chromatin fiber structure map of the human genome that can provide a framework on which to overlay other epigenetic information. It will now be interesting to determine how the features of this map are altered between cell types and between species.

Experimental Procedures

Chromatin Preparation and Nuclease Digestion

A normal human male lymphoblastoid cell line (FATO) was grown in RPMI medium (Gibco) supplemented with 10% fetal calf serum (FCS), MEM nonessential amino acids (Sigma), 2 mM L-Glutamine, 0.5 mM pyruvate, 1 mM oxaloacetic acid, 0.2 units/ml human insulin, penicillin/streptomycin, and 3 mM MOPS. Nuclei were prepared as described (Gilbert et al., 2003) and resuspended in NB-R (85 mM KCl, 10 mM Tris-HCl [pH 7.6], 5.5% (w/v) sucrose, 1.5 mM $CaCl_2$, 3 mM $MgCl_2$, 250 μM PMSF). They were digested with 8–14 units of MNase (Worthington), per 20 A_{260} units of nuclei, for 10 min at room temperature in the presence of 100μg/ml RNaseA. Digestion was stopped by adding EDTA to 10 mM. The nuclei were washed, resuspended in a small volume of $TEEP_{20}$ (10 mM Tris-HCl [pH 8.0], 1 mM EDTA, 1 mM EGTA, 250 μM PMSF, 20 mM NaCl), and then incubated at 4°C overnight. Nuclear debris was removed by centrifugation leaving soluble chromatin in the supernatant.

Sucrose Gradient Sedimentation

Soluble chromatin was fractionated using sucrose gradient sedimentation (Noll and Noll, 1989) in $TEEP_{80}$ (TEEP containing 80 mM NaCl). 400 μl soluble chromatin was loaded on to a 6%–40% isokinetic sucrose gradient and centrifuged at 4°C (41,000 rpm for 2.5 hr in a SW41 rotor). 500 μl fractions were collected from the gradient by upward displacement and the DNA was purified from them by SDS/proteinase K digestion, phenol-chloroform, chloroform extraction, and ethanol precipitation.

Agarose Gel Electrophoresis

DNA from gradient fractions was analyzed by electrophoresis through 0.7% agarose in 1 × TPE buffer (90 mM Tris-phosphate, 2 mM EDTA) with buffer circulation. Preparative fractionation of DNA from gradient fractions was carried out by pulsed-field gel electrophoresis (PFGE) (CHEF system, Biorad) through 1% low melting point agarose in 0.5 × TBE, at 180 V, for 40 hr, with a 0.1–2 s switching time. Size markers were 1 kb (Promega) and 2.5 kb (Biorad) DNA ladders. EtBr-stained gels were scanned using a 473 nm laser and a 580 nm band-pass filter on a Fuji FLA-2000. DNA from transverse gel slices was isolated by β-agarase (NEB) digestion, followed by phenol-chloroform, chloroform extraction, and ethanol precipitation.

Labeling of DNA Fractions

DNA purified from gel slices was either sonicated or digested with Sau3AI. After sonication, the DNA ends were made blunt using mung bean nuclease (NEB). DNAs were ligated to annealed unphosphorylated catch-linkers with either Sau3AI or blunt compatible ends. The Sau3A1 linkers are described previously (Fantes et al., 1995). Blunt-end linkers were the same but with the Sau3AI overhang removed. After ligation, nicks in the top strand were translated using the strand displacement activity of Klenow exo-(NEB). The samples were then amplified by PCR using one of the catch-linker oligonucleotides as primer (30 cycles of 94°C 1 min, 58°C 1 min, 72°C 2 min).

DNA samples were labeled for FISH by nick-translation with either biotin- or digoxigenin-dUTP, or dCTP. DNA samples for micro-array hybridization were labeled by random-prime labeling as previously described (Shaw-Smith et al., 2004).

FISH

200 ng of labeled DNA and the required amount of human Cot1 DNA (Gibco) were hybridized to human metaphase chromosomes as previously described but using 2 days of hybridization (Fantes et al., 1992). Nonspecific hybridization was removed by washing (Gilbert et al., 2003). Cohybridization of cosmid probes from 11p15.5 and a chromosome 11p paint to nuclei prepared from FATO cells was as previously described (Mahy et al., 2002).

Biotinylated probes were detected using sequential layers of avidin-FITC and biotinylated antiavidin. Digoxigenin-labeled probes were detected using rhodamine antidig sheep antibody and Texas Red-antisheep antibody (Vector). Slides were counterstained with 0.5μg/ml DAPI and imaged as previously described (Mahy et al., 2002).

Microarray Hybridization

Hybridization to the 1 Mb and 22q tiling path arrays was performed as described previously (Fiegler et al., 2003), but with slight modification. Cy3 and Cy5 labeled test and control DNAs were combined, precipitated together with 135 μg of human Cot1 DNA (Roche) and 600 μg yeast tRNA (Invitrogen) and resuspended in 30 μl of hybridization buffer. To prehybridize the arrays, 800 μg of herring sperm DNA (Sigma) and 135 μg of Cot1 DNA were resuspended in 45 μl of hybridization buffer and incubated with the array for 1 hr at 37°C under a cover slip. Slides were washed in PBS and spun dry (800 *g*, 1 min) before replacing the prehybridization solution with the hybridization mix. Hybridization was performed under a cover slip for 24 hr at 37°C in hybridization chambers humidified with 20% formamide and 2 × SSC.

Arrays were scanned using an Agilent scanner (Agilent Technologies). Fluorescent intensities were extracted after subtraction of local background using SPOT (Jain et al., 2002). Signal intensities were normalized by dividing the ratio of each data point by the median ratio of all autosomal clones on the array. Any data points falling >2 standard deviations from the mean of color reversal experiments were removed from subsequent analysis. Cytogenetic and map position of BACs on the microarray was established using the NCBI build 34 assembly of the human genome.

Acknowledgments

W.A.B is a Centennial fellow of the James S. McDonnell Foundation. We thank the microarray Core Facility at the Wellcome Trust Sanger Institute for printing the arrays and Douglas Stuart at the MRC HGU for preparation of figures. We thank Jim Allan (The University of Edinburgh) for his continuing advice and Robin Allshire, Howard Cooke, Nick Hastie, and Richard Meehan for their critical reading of the manuscript.

Received: February 3, 2004
Revised: July 8, 2004
Accepted: July 13, 2004
Published: September 2, 2004

References

Bellard, M., Gannon, F., and Chambon, P. (1978). Nucleosome structure III: the structure and transcriptional activity of the chromatin containing the ovalbumin and globin genes in chick oviduct nuclei. Cold Spring Harb. Symp. Quant. Biol. *42*, 779–791.

Belmont, A.S., and Bruce, K. (1994). Visualization of G1 chromosomes: a folded, twisted, supercoiled chromonema model of interphase chromatid structure. J. Cell Biol. *127*, 287–302.

Caplan, A., Kimura, T., Gould, H., and Allan, J. (1987). Perturbation of chromatin structure in the region of the adult β-globin gene in chicken erythrocyte chromatin. J. Mol. Biol. *193*, 57–70.

Caron, H., van Schaik, B., van der Mee, M., Baas, F., Riggins, G., van Sluis, P., Hermus, M.C., van Asperen, R., Boon, K., Voute, P.A., et al. (2001). The human transcriptome map: clustering of highly expressed genes in chromosomal domains. Science *291*, 1289–1292.

Chambeyron, S., and Bickmore, W.A. (2004). Chromatin decondensation and nuclear re-organization of the Hoxb locus upon induction of transcription. Genes Dev. *18*, 1119–1130.

Craig, J.M., and Bickmore, W.A. (1994). The distribution of CpG islands in mammalian chromosomes. Nat. Genet. *7*, 376–382.

Croft, J.A., Bridger, J.M., Perry, P., Boyle, S., Teague, P., and Bickmore, W.A. (1999). Differences in the localization and morphology of chromosomes in the human nucleus. J. Cell Biol. *145*, 1119–1131.

Fan, J.Y., Gordon, F., Luger, K., Hansen, J.C., and Tremethick, D.J. (2002). The essential histone variant H2A.Z regulates the equilibrium between different chromatin conformational states. Nat. Struct. Biol. *9*, 172–176.

Fantes, J.A., Bickmore, W.A., Fletcher, J.M., Ballesta, F., Hanson, I.M., and van Heyningen, V. (1992). Submicroscopic deletions at the WAGR locus, revealed by nonradioactive in situ hybridization. Am. J. Hum. Genet. *51*, 1286–1294.

Fantes, J.A., Redeker, B., Breen, M., Boyle, S., Brown, J., Fletcher, J., Jones, S., Bickmore, W., Fukushima, Y., Mannens, M., et al. (1995). Aniridia-associated cytogenetic rearrangements suggest that a position effect may cause the mutant phenotype. Hum. Mol. Genet. *4*, 415–422.

Felsenfeld, G., and Groudine, M. (2003). Controlling the double helix. Nature *421*, 448–453.

Fiegler, H., Carr, P., Douglas, E.J., Burford, D.C., Hunt, S., Scott, C.E., Smith, J., Vetrie, D., Gorman, P., Tomlinson, I.P., and Carter, N.P. (2003). DNA microarrays for comparative genomic hybridization based on DOP-PCR amplification of BAC and PAC clones. Genes Chromosomes Cancer *36*, 361–374.

Fischle, W., Wang, Y., and Allis, C.D. (2003). Histone and chromatin cross-talk. Curr. Opin. Cell Biol. *15*, 172–183.

Fisher, E.A., and Felsenfeld, G. (1986). Comparison of the folding

of beta-globin and ovalbumin gene containing chromatin isolated from chicken oviduct and erythrocytes. Biochemistry *25*, 8010–8016.

Furey, T.S., and Haussler, D. (2003). Integration of the cytogenetic map with the draft human genome sequence. Hum. Mol. Genet. *12*, 1037–1044.

Ghirlando, R., Litt, M.D., Prioleau, M.-N., Recillas-Targa, F., and Felsenfeld, G. (2004). Physical properties of a genomic condensed chromatin fragment. J. Mol. Biol. *336*, 597–605.

Gilbert, N., and Allan, J. (2001). Distinctive higher-order chromatin structure at mammalian centromeres. Proc. Natl. Acad. Sci. USA *98*, 11949–11954.

Gilbert, N., Boyle, S., Sutherland, H., de Las Heras, J., Allan, J., Jenuwein, T., and Bickmore, W.A. (2003). Formation of facultative heterochromatin in the absence of HP1. EMBO J. *22*, 5540–5550.

Greulich, K.O., Wachtel, E., Ausio, J., Seger, D., and Eisenberg, H. (1987). Transition of chromatin from the "10 nm" lower order structure, to the "30 nm" higher order structure as followed by small angle X-ray scattering. J. Mol. Biol. *193*, 709–721.

Holmquist, G.P. (1992). Chromosome bands, their chromatin flavors, and their functional features. Am. J. Hum. Genet. *51*, 17–37.

Jain, A.N., Tokuyasu, T.A., Snijders, A.M., Segraves, R., Albertson, D.G., and Pinkel, D. (2002). Fully automatic quantification of microarray image data. Genome Res. *12*, 325–332.

Jolly, C., Metz, A., Govin, J., Vigneron, M., Turner, B.M., Khochbin, S., and Vourc'h, C. (2003). Stress-induced transcription of satellite III repeats. J. Cell Biol. *164*, 25–33.

Kim, Y., and Clark, D.J. (2002). SWI/SNF-dependent long-range remodeling of yeast HIS3 chromatin. Proc. Natl. Acad. Sci. USA *99*, 15381–15386.

Kimura, T., Mills, F.C., Allan, J., and Gould, H. (1983). Selective unfolding of erythroid chromatin in the region of the active β-globin gene. Nature *306*, 709–712.

Langmore, J.P., and Paulson, J.R. (1983). Low angle x-ray diffraction studies of chromatin structure in vivo and in isolated nuclei and metaphase chromosomes. J. Cell Biol. *96*, 1120–1131.

Lercher, M.J., Urrutia, A.O., and Hurst, L.D. (2002). Clustering of housekeeping genes provides a unified model of gene order in the human genome. Nat. Genet. *31*, 180–183.

Mahy, N.L., Perry, P.E., and Bickmore, W.A. (2002). Gene density and transcription influence the localisation of chromatin outside of chromosome territories detectable by FISH. J. Cell Biol. *159*, 753–763.

McGhee, J.D., Nickol, J.M., Felsenfeld, G., and Rau, D.C. (1983). Higher order structure of chromatin: orientation of nucleosomes within the 30 nm chromatin solenoid is independent of species and spacer length. Cell *33*, 831–841.

McKittrick, E., Gafken, P.R., Ahmad, K., and Henikoff, S. (2004). Histone H3.3. is enriched in covalent modifications associated with active chromatin. Proc. Natl. Acad. Sci. USA *101*, 1525–1530.

Muller, W.G., Walker, D., Hager, G.L., and McNally, J.G. (2001). Large-scale chromatin decondensation and recondensation regulated by transcription from a natural promoter. J. Cell Biol. *154*, 33–48.

Noll, H., and Noll, M. (1989). Sucrose gradient techniques and applications to nucleosome structure. Methods Enzymol. *170*, 55–116.

Nye, A.C., Rajendran, R.R., Stenoien, D.L., Mancini, M.A., Katzenellenbogen, B.S., and Belmont, A.S. (2002). Alteration of large-scale chromatin structure by estrogen receptor. Mol. Cell. Biol. *22*, 3437–3449.

Rizzi, N., Denegri, M., Chiodi, I., Corioni, M., Valgardsdottir, R., Cobianchi, F., Riva, S., and Biamonti, G. (2004). Transcriptional activation of a constitutive heterochromatic domain of the human genome in response to heat shock. Mol. Biol. Cell *15*, 543–551.

Saccone, S., De Sario, A., Wiegant, J., Raap, A.K., Della Valle, G., and Bernardi, G. (1993). Correlations between isochores and chromosomal bands in the human genome. Proc. Natl. Acad. Sci. USA *90*, 11929–11933.

Schroder, A.R.W., Shinn, P., Chen, H., Berry, C., Ecker, J.R., and Bushman, F. (2002). HIV-1 integration in the human genome favors active genes and local hotspots. Cell *110*, 521–529.

Shaw-Smith, C., Redon, R., Rickman, L., Rio, M., Willatt, L., Fiegler, H., Firth, H., Sanlaville, D., Winter, R., Colleaux, L., et al. (2004). Microarray based comparative genomic hybridisation (array-CGH) detects submicroscopic chromosomal deletions and duplications in patients with learning disability/mental retardation and dysmorphic features. J. Med. Genet. *41*, 241–248.

Shiels, C., Coutelle, C., and Huxley, C. (1997). Contiguous arrays of satellites 1, 3, and beta form a 1.5-Mb domain on chromosome 22p. Genomics *44*, 35–44.

Sun, F.L., Cuaycong, M.H., and Elgin, S.C. (2001). Long-range nucleosome ordering is associated with gene silencing in Drosophila melanogaster pericentric heterochromatin. Mol. Cell. Biol. *21*, 2867–2879.

Tagarro, I., Fernandez-Peralta, A.M., and Gonzalez-Aguilera, J.J. (1994). Chromosomal localization of human satellites 2 and 3 by a FISH method using oligonucleotides as probes. Hum. Genet. *93*, 383–388.

Thoma, F., Koller, T., and Klug, A. (1979). Involvement of histone H1 in the organization of the nucleosome and of the salt-dependent superstructures of chromatin. J. Cell Biol. *83*, 403–427.

Tsukamoto, T., Hashiguchi, N., Janicki, S.M., Tumbar, T., Belmont, A.S., and Spector, D.L. (2000). Visualization of gene activity in living cells. Nat. Cell Biol. *2*, 871–878.

Tumbar, T., Sudlow, G., and Belmont, A.S. (1999). Large-scale chromatin unfolding and remodeling induced by VP16 acidic activation domain. J. Cell Biol. *145*, 1341–1354.

Van den Engh, G., Sachs, R., and Trask, B.J. (1992). Estimating genomic distance from DNA sequence location in cell nuclei by a random walk. Science *257*, 1410–1412.

van Holde, K., and Zlatanova, J. (1996). What determines the folding of the chromatin fiber? Proc. Natl. Acad. Sci. USA *93*, 10548–10555.

Venter, J.C., Adams, M.D., Myers, E.W., Li, P.W., Mural, R.J., Sutton, G.G., Smith, H.O., Yandell, M., Evans, C.A., Holt, R.A., et al. (2001). The sequence of the human genome. Science *291*, 1304–1351.

Vermaak, D., Ahmad, K., and Henikoff, S. (2003). Maintenance of chromatin states: an open-and-shut case. Curr. Opin. Cell Biol. *15*, 266–274.

Versteeg, R., van Schaik, B.D., van Batenburg, M.F., Roos, M., Monajemi, R., Caron, H., Bussemaker, H.J., and van Kampen, A.H. (2003). The human transcriptome map reveals extremes in gene density, intron length, GC content, and repeat pattern for domains of highly and weakly expressed genes. Genome Res. *13*, 1998–2004.

Volpi, E.V., Chevret, E., Jones, T., Vatcheva, R., Williamson, J., Beck, S., Campbell, R.D., Goldsworthy, M., Powis, S.H., Ragoussis, J., et al. (2000). Large-scale chromatin organisation of the major histocompatibility complex and other regions of human chromosome 6 and its response to interferon in interphase nuclei. J. Cell Sci. *113*, 1565–1576.

Weintraub, H., and Groudine, M. (1976). Chromosomal subunits in active genes have an altered conformation. Science *193*, 848–856.

Wolffe, A.P. (1998). Chromatin Structure and Function. (San Diego: Academic Press).

Woodcock, C.L., Frado, L.L., and Rattner, J.B. (1984). The higher-order structure of chromatin: evidence for a helical ribbon arrangement. J. Cell Biol. *99*, 42–52.

Woodfine, K., Fiegler, H., Beare, D.M., Collins, J.E., McCann, O.T., Young, B.D., Debernardi, S., Mott, R., Dunham, I., and Carter, N.P. (2004). Replication timing of the human genome. Hum. Mol. Genet. *13*, 191–202.

Ye, Q., Hu, Y.F., Zhong, H., Nye, A.C., Belmont, A.S., and Li, R. (2001). BRCA1-induced large-scale chromatin unfolding and allele-specific effects of cancer-predisposing mutations. J. Cell Biol. *155*, 911–921.

Yokota, H., Singer, M.J., van den Engh, G.J., and Trask, B.J. (1997). Regional differences in the compaction of chromatin in human G_0/G_1 interphase nuclei. Chromosome Res. *5*, 157–166.